

# Emergence of Groupwise Registration in MR Brain Study

Guorong Wu<sup>1,\*</sup>, Hongjun Jia<sup>1,\*</sup>, Qian Wang<sup>1,2,\*</sup>, Feng Shi<sup>1</sup>, Pew-Thian Yap<sup>1</sup> and Dinggang Shen<sup>1</sup>

<sup>1</sup>Department of Radiology and BRIC  
University of North Carolina at Chapel Hill, NC 27599, U.S.A.  
Email: {grwu, jiahj, fengshi, ptyap, dgshen}@med.unc.edu  
<sup>2</sup>Department of Computer Science  
University of North Carolina at Chapel Hill, NC 27599, U.S.A.  
Email: qianwang@cs.unc.edu

## 1. Background

Modern medical imaging technologies such as Magnetic Resonance Imaging (MRI) [1] offer a safe and non-invasive means of performing clinical diagnosis and research, involving human brain development, aging, and disease-induced anomalies. For reliable estimation of disease related micro-structural difference, accurate deformable image registration plays a key fundamental role in dealing with confounding intra-subject variability in longitudinal studies and inter-subject variability in cross-sectional studies.

**Pairwise Registration:** A plethora of pairwise deformable registration algorithms have flourished in the past two decades, comprehensive surveys of which can be found in [2-6]. In general, the goal of image registration is to estimate the deformation field for warping the subject image (or moving image) to the template image (or fixed image) by maximizing a certain similarity measure between the warped subject and the template. Upon successful registration, intra- or inter-subject differences are minimized, while at the same time disease-related changes and morphological variations are preserved.

The majority of image registration algorithms fall into three categories: landmark-based [7-9], intensity-based [10-15], and feature-based [16-19]. Landmark-based algorithms take advantage of anatomical prior knowledge and are thus computationally fast, since only a few landmarks out of all voxels in an image volume need to be matched. It is however a challenging task even for the trained experts to accurately place a sufficient number of anatomical landmarks for achieving accurate registration. Moreover, inter-rater landmark-placement variability could be large, thus seriously undermining the performance of landmark-based registration algorithms. Intensity-based algorithms

---

\* Guorong Wu, Hongjun Jia, and Qian Wang contributed equally to this book chapter.

take a different approach by aiming to maximize the intensity similarity between a pair of images, which can be fully automated by employing state-of-the-art optimization methods for deformation field estimation. However, intensity similarity does not necessarily imply anatomical correspondence. In light of this, feature-based algorithms formulate image registration as a problem of feature matching for deformation estimation. Anatomical correspondences identified by feature-based registration have been found to be more reliable than those based on intensity alone.

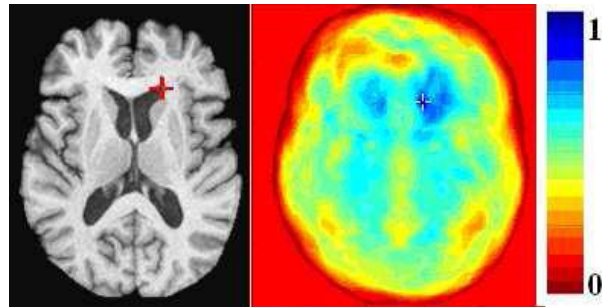


**Fig. 1.** Color-coded map (right) of the degree of similarity between the attribute vectors of the marked point (the red cross in the left image) and every other point in the brain. Blue denotes for high similarity and red for low similarity [17].

HAMMER (Hierarchical Atttribute Matching Mechanism for Elastic Registration) [17, 18] - one of the most popular brain MRI registration algorithms - integrates the advantages of the methods from all three categories, and alleviates their limitations. HAMMER designates an attribute vector to each image point as its morphological signature for efficient determination of anatomical correspondences between an image pair. The attribute vector consists of a variety of image derived features, including image intensity, edge type, and geometric moment invariants (GMIs) [20] computed for three types of tissues, i.e., white matter (WM), gray matter (GM), and cerebrospinal fluid (CSF). The degree of similarity between the GMI-based features of a particular point at the anterior horn of the left ventricle (as indicated by a red cross) and the attribute vector of every other point in the image is color-coded and shown in Fig. 1, where blue denotes high similarity and red otherwise. To achieve robust registration and to avoid local minima, only a small number of the voxels with the most distinctive attribute vectors - the driving voxels - in both template and subject are selected for guiding the initial registration. As registration progresses, an increasing number of voxels are selected as driving voxels to refine the deformation field. Fig. 2 illustrates the hierarchical deformation mechanism in HAMMER with points in red, green, and yellow denoting the driving voxels identified in the initial, middle, and

final registration stages, respectively. The gradually refined deformation field is shown in the bottom of Fig. 2.

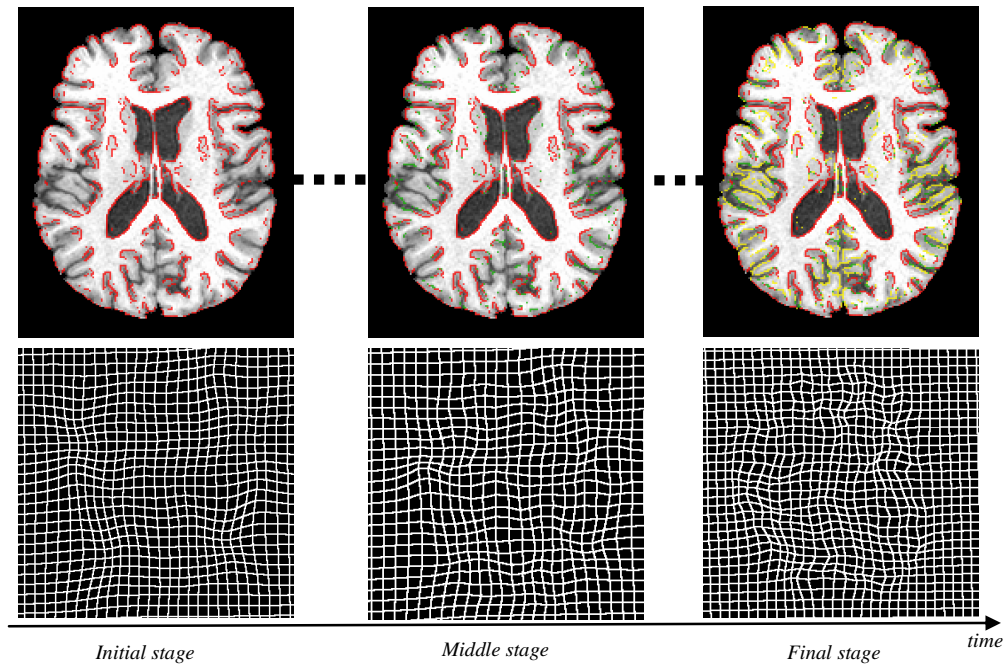


**Fig. 2.** Hierarchical selection of the driving voxels, and evolution of deformation fields in different registration stages [19]. In the initial stage, only a small number (around ~2% of total voxels) of voxels with distinctive attribute vectors (displayed in red), located at sulcal roots, gyral crowns, and ventricular boundaries, are selected to steer the registration of other less distinctive voxels. As registration progresses, more and more voxels are selected as the driving voxels, as shown in green and yellow, respectively. The bottom row shows the corresponding deformation fields estimated at three different stages. It can be observed that, as the number of the driving voxels increases, the deformation field is gradually refined.

HAMMER has been evaluated in a number of brain studies and is found to achieve relatively high accuracy, even in the presence of significant morphological differences in cortical regions. In Fig. 3, some representative registration results of elderly subjects from the Baltimore Longitudinal Study of Aging (BLSA [21]) are shown to demonstrate the performance of HAMMER. The abundance of anatomical details retained in the average image gives a good indication of HAMMER’s capability in registering images with significant structural variations.

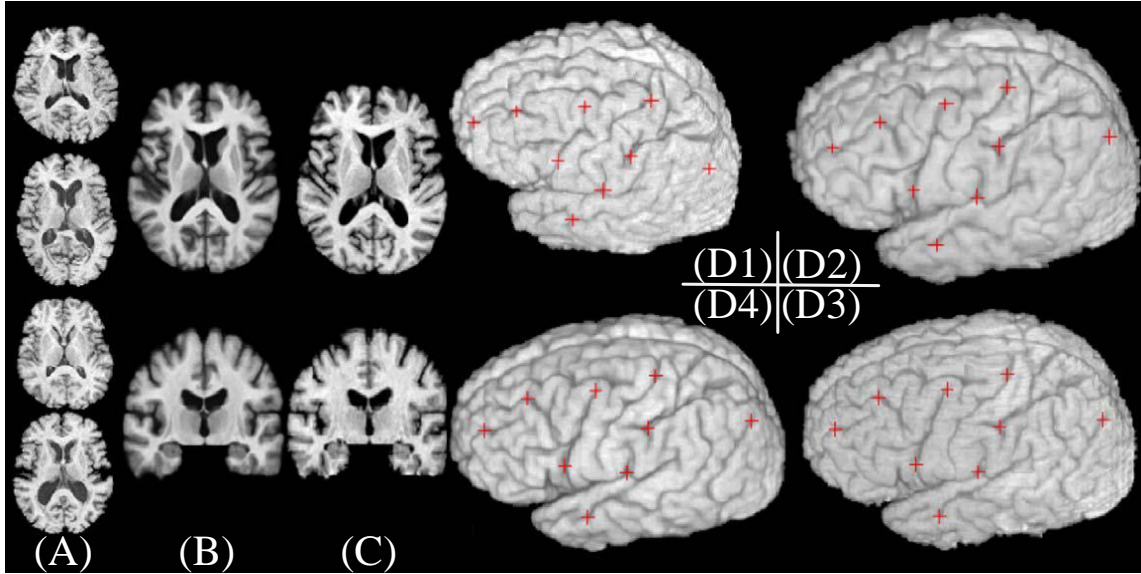


**Fig. 3.** Results from HAMMER algorithm [22]. (A) Four representative cross sections from BLSA dataset; (B) Representative views from the average of the 18 images after normalization onto the template in (C) by HAMMER; (D1-D4) The 3D rendering of a representative case, its warped configuration using HAMMER, the template and the average of 18 warped brains, respectively. The anatomical details seen in (B) and (D4) are the evidences of the registration accuracy. The red crosses in (D1-D4) are identically placed to allow for visual inspection of point correspondences.

**Limitations of Pairwise Registration:** Due to the high anatomic variability among individual human brains, any atlas or clinical diagnostic system based on a single subject’s anatomy cannot achieve full success [23]. Although it is applicable to register each subject to the template by pairwise registration for the intra- or inter-population analysis, registration schemes based on a single reference will introduce systematic bias towards the shape of the selected template. To increase the signal-to-noise ratio (SNR) in subsequent statistical analysis, the registration of a large number of images from different individuals needs to be considered within a unified registration framework, so that the overall registration accuracy for all images in a population can be maximized. Eventually, the anatomical shape differences within and across populations can be better delineated. Thus, groupwise registration algorithms which avoid bias in template selection are recently gaining increasing research interest.

**Emergence of Groupwise Registration:** To alleviate limitations of pairwise registration, groupwise registration aims to warp all images towards the common space by simultaneously estimating their deformations [24-43]. In other words, given an image population  $I = \{I_i | i = 1, \dots, N\}$ , the ultimate

goal of groupwise registration is to find a set of deformations  $\mathbf{T} = \{T_i | i = 1, \dots, N\}$  to minimize the variation within the registered subject set  $\tilde{\mathbf{I}} = \{T_i(I_i) | i = 1, \dots, N\}$ . The scheme of groupwise registration is illustrated in the left panel of Fig. 4. Specifically, subject  $I_i$  is warped to the common space, following the corresponding deformation  $T_i$ . The estimated deformation usually complies with the constraint of invertibility. Then, any two subjects can be connected via the common space. For example, in the right panel of Fig. 4, subject  $i$  can be warped onto the space of subject  $j$  by a composed transformation and, i.e.,  $T_j^{-1} \circ T_i$ . After all images have been aligned in the common space, any quantitative analysis can be performed.

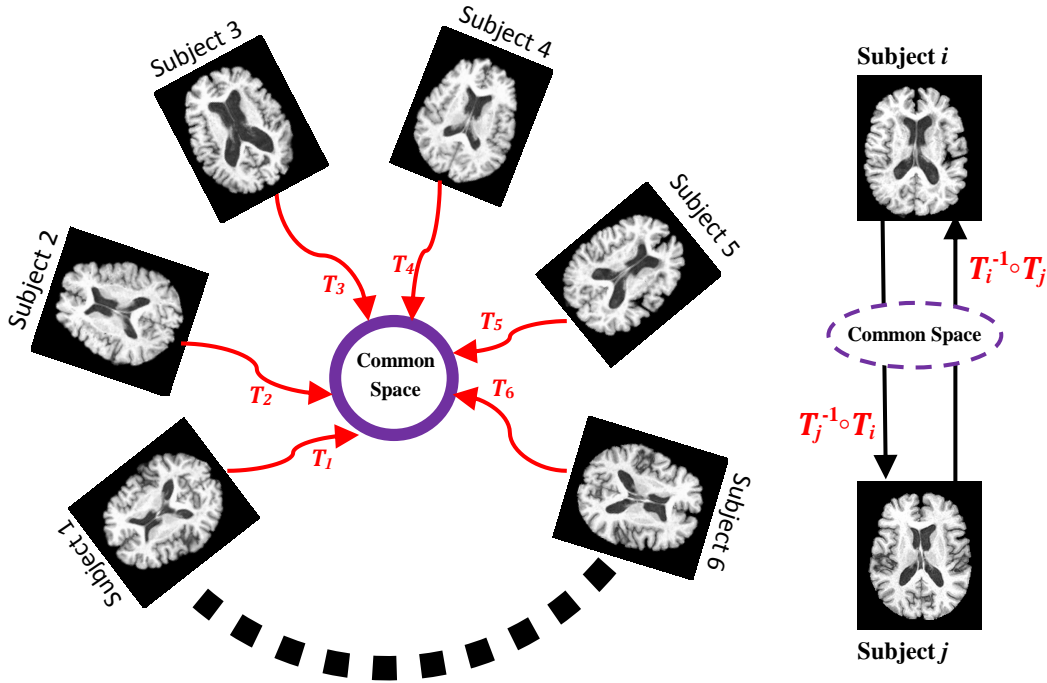


**Fig. 4.** In groupwise registration, all subjects are warped onto a common space by following their individual deformations (as indicated by red arrows). Also, any subject  $I_i$  is connected to another subject  $I_j$  via the common space by a composed transformation, i.e.,  $T_j^{-1} \circ T_i$ , as shown in the right panel.

The majority of the current groupwise registration algorithms can be classified into three classes: 1) pairwise registration derived groupwise registration [24, 25]; 2) population center guided groupwise registration [26, 27, 32, 33, 38, 40, 42]; and 3) hidden common space based groupwise registration [28-30, 36, 37, 44]. The first class of methods directly applies pairwise registration to achieve the goal of groupwise registration. They attempt to determine an unbiased or least biased atlas by exhaustive pairwise registration of image pairs in a group. We will describe two typical methods of this class in

Section 2. Recent groupwise registration algorithms take a different approach by simultaneously estimating the deformations in relation to a common space. Specifically, the second class of methods estimates the population center by explicit registration of each subject image to a group mean image. The third class of methods formulates the groupwise registration as an optimization problem with an objective function that drives all subjects towards the hidden common space. We will describe with more details these two classes of groupwise registration algorithms in Section 3 and Section 4, respectively. The major difference between the last two classes of methods is that, in the second class, the image in the common space is determined explicitly and is evolved with further registration, while in the third class, the image in the common space is implicit or hidden throughout the optimization. We will provide several typical applications of groupwise registration in Section 5, including image parcellation [22], multiple modal image population exploration [31], and infant atlas building [45].

## 2. Pairwise Registration Derived Groupwise Registration

One of the most straightforward ways of achieving groupwise registration is to apply the pairwise registration directly on the images in the population. In this section, we briefly introduce two such groupwise registration algorithms. Seghers et al. [25] proposed to construct the brain atlas based on exhaustive pairwise registration, with possible number of registration totaling up to  $N(N - 1)$ . By taking in turn every image  $I_i$  in the group as the template, they estimate the deformation fields to all other  $N - 1$  images with respect to the template, and then warp the template with the average deformation field. Then the final atlas is obtained by the voxelwise averaging of all warped images. However, this method suffers from very heavy computation cost. For example, it takes about 170 days on one 2.6GHz processor to perform 4032 pairwise registrations for a group of 64 subjects [25].

An alternative method can be found in the work of Park et al. [24]. They perform pairwise registrations among  $N$  subjects by taking each subject as a template in turn and registering the rest of the subjects onto this template. Next, instead of averaging all deformed images in [25], they build an  $N \times N$  distance matrix with each element denoting a measure of the bending energy of a particular deformation field. Multidimensional scaling (MDS) [46] is performed on the distance matrix to choose the image that is the closest to the population center as the template. Since the distance matrix is assumed to be symmetric, this method is faster since only  $N(N - 1)/2$  times of pairwise registration need to be performed. Once the least biased template is determined (which is only an approximation to

the real population center), all other images can be mapped onto the template space directly using a pairwise registration method. However, the potential bias introduced in the selection of the template, as well as the difficulty in registering images with large deformations to the selected template, limit its application in practice.

In brief, the goal of this kind of method is to construct an unbiased or least biased atlas. However, the large number of required rounds of pairwise registration limits their application. Possible solution to this is discussed next.

### **3. Population Center Guided Groupwise Registration**

Groupwise registration can be implemented by aligning all images to a population center. In the literature, several groupwise registration methods have been proposed to better estimate and utilize the population center. For example, the group mean method and its extensions [26, 40, 41] repeatedly estimate the group mean image from the tentatively aligned images and update the deformation of each subject to the newly-estimated group mean image. In the tree-based algorithms [27, 42], all subjects in the population are connected by a tree structure with the root subject considered as the population center. Thus all other subjects can be registered to the root by following the path from each individual node to the root node. To better utilize the local and global information of the manifold spanned by all subjects, a method called Atlas Building by Self-Organized Registration and Bundling (ABSORB) [32, 33] has been proposed recently. In general, ABSORB warps each subject towards its selected neighbors and assures that all subjects can reach the population center. All these algorithms are detailed next.

To avoid the potential bias in groupwise registration, Joshi et al. [26] proposed to solve the groupwise registration in an iterative manner by estimating the population center via the Fréchet mean of all images. An interim population center is first built by averaging all linearly aligned images. And then all images are warped to this interim population center by a diffeomorphism registration framework. The interim population center is further updated based on all tentatively warped images, and then the deformations for all images can be refined as well. The two steps of (1) estimating population center and (2) registering images to the population center are interleaved and iteratively performed. As illustrated in Fig. 5, this method can provide an unbiased population center, and converge fast by a few

iterations. However, the registration process of this method could be misled when trying to register individual images (with sharp anatomical structures) to a blurry group mean image (with ambiguous anatomical structures), due to the difficulty in establishing the reliable correspondences between them, especially in the beginning of the registration.

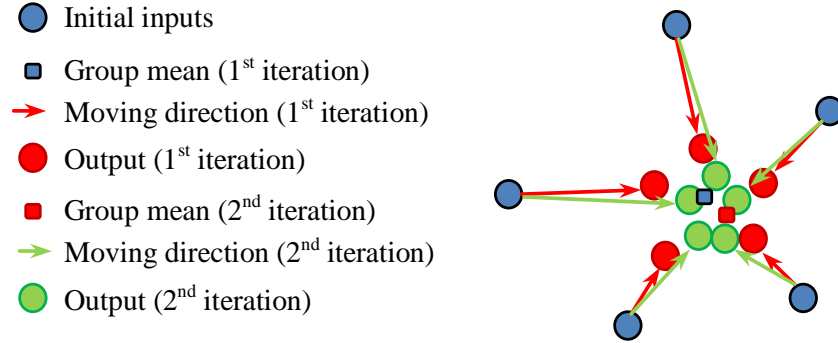


**Fig. 5.** Illustration of the framework of the group mean method. In each iteration, the subjects are warped towards the tentatively estimated group mean. And the group mean is refined based on newly warped subjects.

It is worth noting that other registration methods are also applicable to the group mean framework. For example, Marsland et al. [38] introduced a Minimum Description Length (MDL) based method, which plays as a role similar to the diffeomorphism registration method in [26], for groupwise registration. In MDL, the image population is described by not only a single mean image, but also a set of deformations and a set of residuals, which are encoded according to any given model (e.g., the histogram of the mean image). Based on the information theory, groupwise registration is accomplished when the description length of the population coding is minimized.

Fletcher et al. [40] extended the definition of the geometric median (or the  $L^1$  estimator) to the Riemannian manifold, by adopting geodesic distances between subjects on the manifold and minimizing the distance via gradient based optimization. The geometric median serves as the population center to guide the subsequent registration. They further proved that the geometric median exists and is unique for any non-positively curved manifold or under certain conditions for positively curved manifolds. In their experiments, this extension was demonstrated to be more robust to outliers than the Fréchet mean used by Joshi et al. [26].

Recently, Wu et al. [41] extended the pairwise HAMMER algorithm [17] to work in a groupwise manner. Instead of simply averaging over the intensities of the cohort of images, they proposed to average images region-by-region according to local anatomical shapes. Starting from an exemplar image which has the minimal distance to all other images, more and more anatomical details are gradually augmented to the mean image as registration progresses. In this way, the mean image can be kept sharp throughout the whole registration process, which is very important to obtain accurate registration results. In their method, each subject is treated differently (according to the alignment of local anatomical structures) in constructing the group mean based on the alignment of local anatomical shape. Two major advantages are demonstrated: a) the group mean image has minimal anatomical difference to all subjects, and b) the group mean retains the population information as well as sharp anatomical structures.

It is generally difficult to achieve good registration by directly registering each image to a fixed population center, especially when cross-subject anatomical variation is large. Some algorithms have been proposed to warp the individual images with the help of intermediate template [47-50]. These intermediate templates are produced to pave the path for connecting an individual image to the population center. The final registration result can be obtained by deforming each individual image along its respective path to the population center. This idea is applied to the groupwise registration by building a minimum spanning tree (MST) [51] where each node corresponds to one image and each edge indicates the distance between two connected nodes. The root node of the MST, namely the population center, can be determined by selecting a node that has the minimal edge length to all other nodes or that has the maximal number of children. In Hamm et al. [27], after learning the intrinsic manifold of the whole dataset, the population center is determined as the pseudo-geodesic median image since it minimizes the total path length from each image to the template. The corresponding geodesic paths between individual images and the population center are computed to construct a tree based on the learned manifold. The large deformation between the subject and the population center is thus decomposed into several small ones, and the accuracy of registration is improved. Nevertheless, since the population center is approximated by a fixed image (i.e., the root image) from the dataset, the bias is unavoidable in this scenario.

More recently, a new framework for groupwise registration, termed as Atlas Building by Self-Organized Registration and Bundling (ABSORB), was proposed [32, 33]. The basic idea of ABSORB

is illustrated in Fig. 6. This method explores the intrinsic distributions of subjects to guide the registration. The groupwise registration problem is resolved in an iterative manner by warping each image in the population step-by-step on the learned manifold, and, at the same time, maintaining the global distribution of the population. To achieve this goal, two new strategies, namely self-organized registration and image bundling are employed. Specifically in the self-organized registration, each image is warped towards a subset of its neighbors that are closer to the population center, in order to condense the global distribution of the population on the manifold. The tentative population center is updated iteratively and used only to guide the selection of qualified neighbors, thereby not directly involved into registration. After several iterations, some nearby subjects become close enough to each other and are thus bundled together spontaneously into a subgroup. Then ABSORB jumps to the higher level, where the registration is performed on a much smaller dataset which consists of only the representative images of all subgroups. As the result of this hierarchical registration process, a pyramid of images is built automatically and the population center can be eventually generated once the registration arrives at the upmost level. With ABSORB, the possible registration error can be greatly reduced by only warping each individual subject to its neighbors with similar structures. Also, it can produce a smoother registration path, which traverses each subject image to the final population center, than other groupwise registration methods.

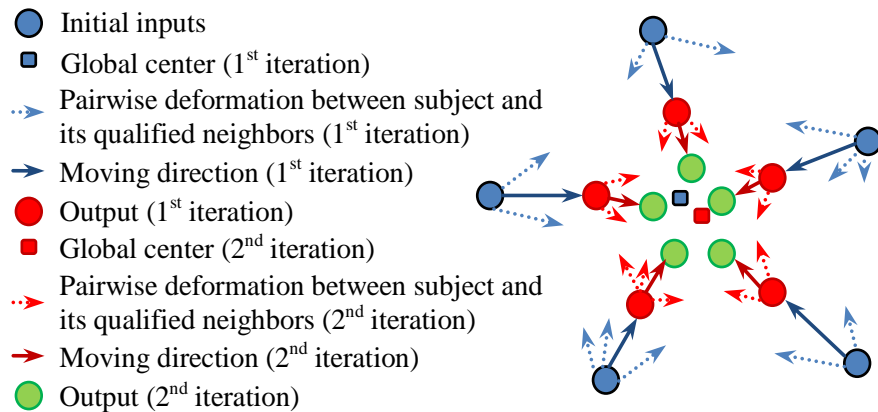


**Fig. 6.** Illustration of the ABSORB [33] framework. In each iteration, each subject is deformed towards its selected neighbors, which are closer to the population center. The estimated population center is updated iteratively based on the tentatively warped images.

Similar to other approaches that solve the groupwise registration in a “relay” fashion [26, 27, 42], the complete path from each individual image to the final population center built by ABSORB is composed of a series of small segments. But ABSORB is inherently different from those methods in

three ways. First, in ABSORB, no fixed intermediate templates are used for any image in any iteration. Instead, the movement of each individual image on the manifold is driven only by a selected set of its qualified neighboring images, not by a common explicit or implicit template. Second, the number of qualified neighboring images is adaptively determined according to the intrinsic data structure learned online, and the complete path generated from each image to the population center on the manifold is generally smoother and more conservative as ABSORB always warps one image to its nearby location, instead of moving to the population center directly. One example is demonstrated in Fig. 7. In contrast, in [26, 27, 42], the direction and the amount of deformation for each image in each iteration are determined by only the selected tentative template, which can often result in a zigzag path if the selected template does not represent the data distribution very well. Finally, the registration path for each image provided by ABSORB is not pre-determined before the actual registration starts. In other words, it is a fully data-driven groupwise registration method. On the contrary, a tree in [27, 42] is built in the pre-processing step and fixed during the whole registration process.

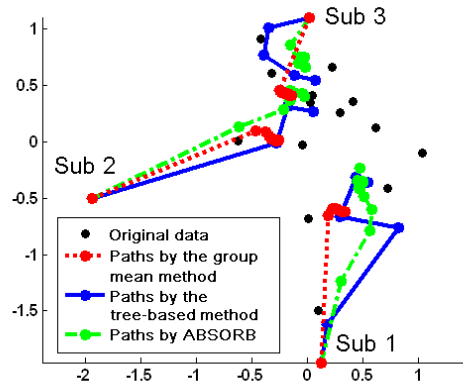


**Fig. 7.** The registration paths produced by three different methods [33]. The paths generated by ABSORB (with green dashed curves) are much smoother than the tree-based method (with blue solid curves), and the paths given by the group mean method (with red dotted curves) show that there is not much progress after the first iteration of registration.

The information provided by the population center has been demonstrated to be very useful in groupwise registration. But due to the huge gap between the limited number of available subjects and the extremely high dimensions of the data space, it is usually very difficult to estimate the population center robustly, and thus an inaccurate population center might lead the whole registration off the track and degrade the statistical analysis that follows.

#### 4. Hidden Common Space Based Groupwise Registration

For the algorithms illustrated in Section 3, groupwise registration is achieved under the guidance by either the selected individual image (such as the root image in the tree-based method) or the group mean image (such as the average of all aligned subjects in [26]). However, both have their limitations. For the former, the difference between the selected individual subject and the real population center cannot be simply ignored even though it might be very close to the real population center. For the latter, since the subjects are far from the good alignment in the initial stage of registration, the tentative mean image by simply averaging all the warped subjects is inevitably fuzzy. Though the mean image guarantees the generation of an unbiased atlas, registration performance might be undermined by the fuzzy mean image due to the lack of structural details for proper correspondence detection.

One common characteristic of the groupwise registration methods described in Section 3 is that they all need explicit approximations of the population center. However, explicit estimation of the population center is not a necessity when the goal of groupwise registration is to estimate the deformation fields for warping each subject to a common space. Given a set of images, a unified objective function is developed to help warp all images to a hidden common space, in which the variation within the subject images w.r.t. deformation fields is minimized. As a result, the estimated deformations for all subjects, which are usually defined in the common space, convey the anatomical diversity across population. The advantage of this kind of groupwise registration algorithm is that it bypasses the estimation of population center by introducing a hidden common space, making the group mean only a by-product of the groupwise registration. In the following, we will summarize several groupwise registration algorithms belonging to this category.

In hidden common space based groupwise registration, pairwise registration cannot be directly applied since there is no paired relationship between any given image and the specific template. In fact, all images need to be warped to an undetermined destination simultaneously, until they are close enough to each other and converge to a hidden common space. In general, a global objective function is defined to minimize the variation between all to-be-registered images. When the objective function is gradually minimized, the images are progressively pushed to converge to the hidden common space. Therefore, groupwise registration can be regarded as a typical optimization problem, with the optimal solution to the deformations for all images estimated by minimizing the objective function.

The ‘‘congealing’’ method proposed by Miller et al. [28, 44] is among the first methods introduced for groupwise registration. In congealing, all images are piled together from top to bottom. Then intensities of the same locations from different images are sampled to form a sequence or a stack, as in the left panel of Fig. 8. If all input images were identical, the intensity values inside the stack would be the same. The aim of the registration algorithm is then to reduce voxel variation within a stack by minimizing the stack entropy. The local variation measurement, namely stack entropy, is further integrated over the whole image domain to obtain a unified objective function. Given the image set  $\mathbf{I}$  and the corresponding (tentative) deformations  $\mathbf{T}$ , the objective function  $f$  can be defined as:

$$f = \int \mathcal{H}(\mathbf{I}(\mathbf{T}(x))) dx, \quad (1)$$

where  $\mathcal{H}$  calculates the entropy over the sequence of intensity values sampled from location  $x$  of all images. By minimizing  $f$ , the optimal estimation of the deformations  $\mathbf{T}$  can be obtained. Without loss of generality, the notation  $\mathbf{T}$  will be omitted in the following for convenience, by assuming that the image set  $\mathbf{I}$  is the tentatively warped results based on the currently-estimated deformations  $\mathbf{T}$ .

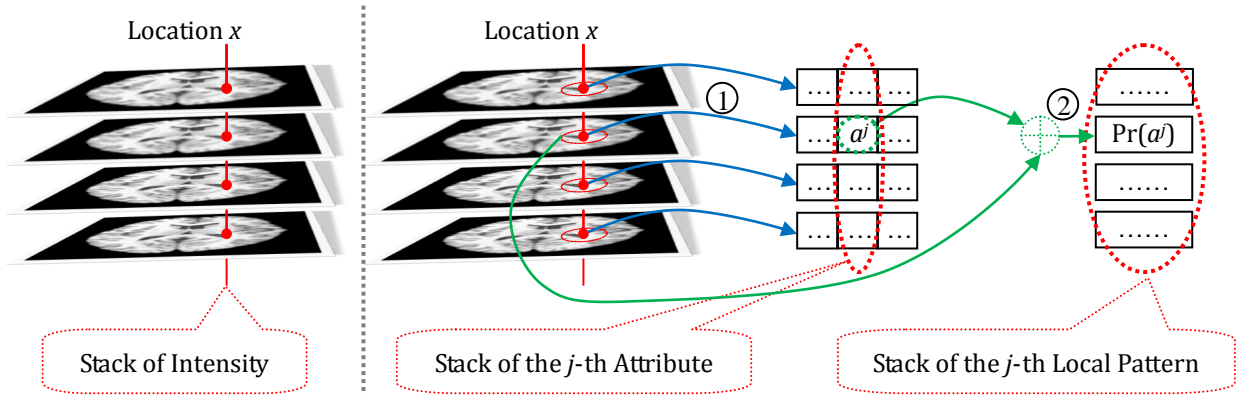


**Fig. 8.** In the left panel, a stack of intensities is sampled from the identical locations of different images [37]. In the right panel, not only the single intensity but also more attributes are sampled to form an attribute vector as a morphological signature of each voxel. Moreover, the neighborhood of each voxel is considered as a local pattern, described by the local probability density function, to construct a robust objective function.

An easy way to calculate the entropy of a finite intensity sequence is to adopt the widely-used Shannon entropy, although some other measurements, such as the variance in the stack, can also be used. In the case of groupwise registration, the stack sampled at location  $x$  consists of the sequence  $\{I_1(x), I_2(x), \dots, I_N(x)\}$ . However, the number of samples in a stack is very limited, posing great

challenge to the accurate estimation of entropy. To alleviate this problem, Parzen window is often used to transfer the discrete sequence into a continuous Gaussian mixture model (GMM). The Gaussians of each GMM, corresponding to individual location  $x$  in the image space, center at the sampled pixel values, respectively. Then the cost function can be represented by:

$$f = - \int \frac{1}{N} \sum_{i=1}^N \log \frac{1}{N} \sum_{j=1}^N G_{\sigma} (I_i(x) - I_j(x)) dx, \quad (2)$$

where  $G_{\sigma}$  is the Gaussian kernel with variance  $\sigma$ .

The deformation can be parameterized in various ways, the choice of which is often closely related to the optimization. The linear part of the deformation is usually the rigid or affine transformation, while the nonlinear part can be described by a dense deformation field. The congealing method implemented in [29] was based on affine transformations, and was then further extended nonlinearly in [30] by modeling the deformation with B-Splines [52]. For optimization, the common approach is to determine the gradient of the objective function with respect to the deformation parameters, and then search for the optimal solution along the steepest descent direction.

For example, in Wang et al. [34], where a group of point-sets are to be registered, each point-set is modeled as a continuous probability density function using Gaussian mixture model (GMM). The Jensen-Shannon (JS) divergence [53] is then used to measure the variation within the group of probability density functions. An objective function is built and further minimized using any gradient-based optimization for estimation of the deformation for each image.

We further note that intensity alone is insufficient for conveying all information needed by registration. It has been proven that attribute vector, consisting of additional information on top of intensities, can better represent each voxel in an MR image. In HAMMER [17], for example, GMIs are used to determine a set of driving voxels for steering the registration. In fact, many types of features which have been shown to be effective descriptors can be incorporated as attributes for medical image registration.

Wang et al. [36, 37] developed a method which integrates the attribute vector into the groupwise registration cost function. Ideally, different attributes in the attribute vector can contribute independent piece of information which is conducive for registration. In Wang et al.'s work [36, 37], both intensity

and intensity gradient are used as attributes for guiding groupwise registration. Intensity gradient is more sensitive than intensity alone to the subtle mismatch of anatomical boundaries. In the very beginning of registration, the variation within the population of images is high. Therefore, the contribution from intensity gradient is weighted less than that of intensity. As registration progresses, the mismatch between any two images becomes lesser. Then, to increase the accuracy in registration, the weighting for contribution of intensity gradient is increased, with simultaneous decrease in contribution from intensity. It is worth noting that, although only intensity and intensity gradient are used as attributes in Wang et al. [36, 37], the framework is flexible enough to accommodate other features for guiding registration.

To further improve the robustness and accuracy of groupwise registration, local pattern is introduced in Wang et al. [36, 37]. In particular, given a center voxel in the specific image, its neighborhood is viewed as a local pattern, as in the right panel of Fig. 8. A Gaussian mixture model is estimated to characterize the local pattern. Suppose  $a^j$  is the  $j$ -th attribute under consideration, then the local pattern centered at location  $x$  in image  $I_i$ , denoted as  $\Pr(a^j|i, x)$ , is defined as:

$$\Pr(a^j|i, x) = \frac{1}{K} \sum_{\Delta x} G_{\sigma}(a^j - a_{i, x+\Delta x}^j), \quad (3)$$

where  $K$  is the total number of voxels in the neighborhood and  $\Delta x$  is the allowable offset in the neighborhood.

A single stack now actually connects a set of local patterns. These local patterns are from different images, but centering at the same locations. The variation within the stack of local patterns can be measured with the JS divergence:

$$JS(x, j) = \mathcal{H} \left( \sum_{i=1}^N \pi_i \cdot \Pr(a^j|i, x) \right) - \sum_{i=1}^N \pi_i \cdot \mathcal{H} \left( \Pr(a^j|i, x) \right). \quad (4)$$

By integrating the JS divergence across the image domain and combining together contributions of different attributes, the final cost function can be formulated. Similarly, gradient based optimization methods can be used to minimize the cost function.

In general, hidden common space based groupwise registration can be formulated as an optimization problem with the goal of minimizing variations within the image population. The way of constructing the objective function varies with applications, and should be further explored in the future. By

avoiding introducing an explicit image in the common space, results yielded by groupwise registration towards the hidden common space can potentially get rid of bias introduced by inappropriate selection of template.

## 5. Applications

Image registration plays a key role in medical image analysis [23, 54]. It can be used to concurrently normalize all subjects in a population, and to propagate labels from template to individual subjects. The deformation field generated from registration records the displacement of corresponding voxels between subject and template, which characterizes the global and local morphological differences. In 4D studies [55, 56], the longitudinal changes measured by the registration algorithm can be used to reveal the patterns related to brain development, aging, and neurologic or neuropsychiatric disorders. The use of groupwise registration for morphological measurement has multiple advantages. First, it needs no selection of template, thus avoiding possible bias in data analysis. Second, it is able to generate more representative group mean. Groupwise registration can be easily incorporated into most applications by using it to replace the pairwise registration, for achieving more powerful and unbiased analysis of data. We will present three typical applications of groupwise registration in this section, besides pointing out other possible applications.

**Typical Applications:** Deformable image registration serves multiple roles in many clinical studies. One of the most popular applications is the evaluation of anatomical variability in human population. By registering each individual subject to a template, a dense deformation field can be obtained, encoding dilation and contraction information of regions of each subject with respect to the template. Therefore, these deformation fields offer ways for pathology detection, identification of gender-specific anatomic patterns, and mapping of dynamic patterns of structural changes in disease-related neuro-developmental and degenerative processes. Taking HAMMER as an example, Fig. 9 demonstrates several typical clinical applications requiring registration of the subject images to the template image (in Fig. 9 (A)). These applications are further illustrated in Fig. 9 (B1-B7).

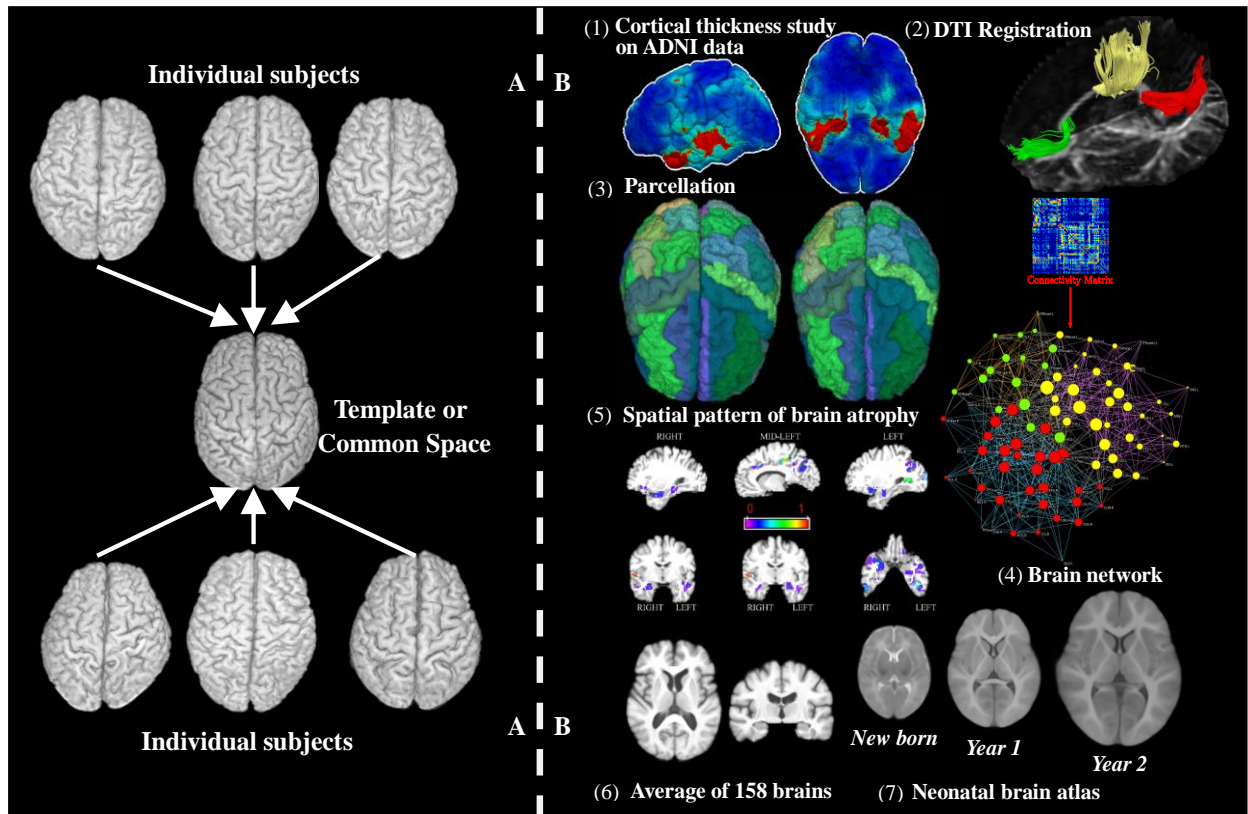


**Fig. 9.** Illustration of various applications of image registration. Panel (A) shows the procedure of warping individuals subjects (top and bottom rows) to the template (in a pairwise scenario) or common space (in a groupwise scenario). After spatial normalization, numerous clinical applications can be performed, with some typical ones shown in the right panel (B). From (B1) to (B7), we show the illustrative results of (B1) cortical thickness study on ADNI data, (B2) DTI registration, (B3) image parcellation, (B4) brain network discovery on structural images, (B5) spatial pattern of brain atrophy with respect to MCI, (B6) normalization of elderly brains, and (B7) study on infant brain development, respectively.

1. After registering all subjects to the template space, subtle changes of cortical thickness [57, 58] during pathological or physiological development can be captured, providing a powerful tool for diagnosis and study of a variety of neuro-degenerative and psychiatric disorders [59]. (B1) shows the left and interior views of statistical significance ( $p$ -value) of the correlations detected between the thickness and the CDR-SOB scores.
2. Diffusion tensor imaging (DTI) provides unprecedented insight into brain white matter structures and is commonly used to delineate subtle abnormalities caused by diseases, including stroke, multiple sclerosis, dyslexia, and schizophrenia. HAMMER has also been extended to DTI image

registration [60, 61]. (B2) demonstrates the aligned fiber bundles in the genu, splenium, and body of the corpus callosum in green, red, and yellow respectively.

3. Registration can be used to automatically parcellate and label the brain structures for individual brain images after estimating the deformation field between the subject and the template [22]. (B3) shows 3D renderings of the label map and a representative labeling of an individual's brain after registration to the template. It is worth noting that features extracted from the volumetric measurements of labels can also be used to classify the normal controls and diseased patients.
4. The human brain is considered as a collection of interacting networks with specialized functions to support various cognitive tasks [62]. The connectivity also changes as a consequence of the neuron degeneration, either from natural aging or diseases such as Alzheimer's Disease. After the registration and parcellation on DTI images, the connectivity of two ROIs can be identified by the common traversing fibers. This connectivity information is encoded in a connectivity matrix (in the top of (B4)). After properly thresholding the connectivity matrix, a brain network can be obtained, where the spring-embedding visualization is displayed in the bottom of (B4).
5. Computer-based pattern classification of MRI is able to detect patterns of brain structure characterizing subtle anatomical difference between normal and patient subjects after image registration. (B5) shows the representative cross-sections highlighting the brain regions that collectively form a spatial pattern of brain atrophy that is highly indicative of mild cognitive impairment (MCI) [63]. The color coding shows the relative importance of a brain region for classification.
6. HAMMER has been used as the key registration method in one of the most comprehensive longitudinal studies of aging in the world to date (Baltimore Longitudinal Study of Aging – BLSA [21]), in which HAMMER has successfully processed ~2100 images. Because of the high accuracy of HAMMER (as the sharp average image of all normalized subjects shown in (B6)), we can now localize longitudinal atrophy and detect abnormal anatomical changes with better spatial specificity and sensitivity.
7. Study of early brain is very challenging because of the insufficient image resolution, low SNR, dynamic myelination of white matter, and lack of prior knowledge. (B7) shows the atlases of new born, year 1, and year 2 infants built from the well aligned subjects, which facilitate the infant brain analysis, such as atlas-based tissue segmentation, and brain network construction [42, 45, 64-66].

**The Advantages of Groupwise Registration:** We demonstrate here the performance gain of groupwise registration over pairwise registration, i.e., HAMMER (source code available at <http://www.nitrc.org/projects/hammerwml/>). Groupwise registration algorithms used in the comparison are the group mean algorithm [26], ABSORB [32, 33], and the congealing algorithm [30]. Additionally, we provide the comparison results for the hierarchical groupwise registration algorithm presented in [43], which utilizes the congealing method [30] in the implementation of each level.

We first evaluate these five algorithms on 18 elderly brains from the BLSA dataset [21] by comparing the overlap ratio on white matter (WM), gray matter (GM), and ventricle (VN). Here we use the Jaccard Coefficient metric [67] to measure the alignment of two regions with the same tissue. For the two registered regions  $A$  and  $B$ , the Jaccard Coefficient is defined as:

$$J(A, B) = \frac{|A \cap B|}{|A \cup B|}, \quad (5)$$

where  $|\cdot|$  denotes the number of voxels in the underlying region. To evaluate registration accuracy, we employ a majority vote approach by assigning each voxel with a tissue label that is the majority returned by all tissue labels at the same location of all the aligned subjects. Then the Jaccard Coefficient between each of the registered label images and the voted label will be calculated. It is worth noting that this is a very strict definition for measurement of ROI overlap, and it emphasizes the importance of groupwise registration in measuring the group performance. In the following experiments, we use the average score of Jaccard Coefficients as the overlap ratio for each tissue label.

Fig. 10 shows a group of 18 elderly brain images. Each image is of size  $256 \times 256 \times 124$  and resolution  $0.9375 \times 0.9375 \times 1.5mm^3$ . It can be observed that the anatomical structures vary a lot across different subjects, especially for the ventricle and the cortex. To better evaluate the performance of pairwise registration (by HAMMER), we randomly select five individual subjects (shown by red boxes in Fig. 10) as templates in reporting both the mean and standard deviation of the overlap ratios over three different tissues (the first row of Table 1).

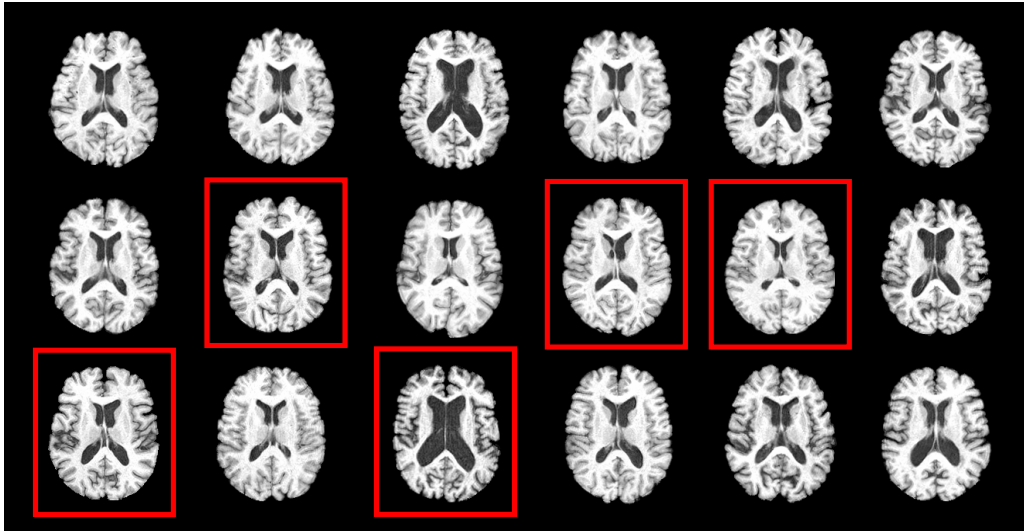


**Fig. 10.** 18 elderly brain images used in evaluation of three registration methods. The five subjects with red rectangles are selected as template images in the pairwise registration algorithm for a fair performance evaluation of the pairwise registration algorithms.

The overlap ratios on WM, GM, and VN, as well as the overall overlap ratio on the whole brain by different groupwise methods are displayed from the second to fifth row in Table 1. It can be observed that the second class (i.e., the population center guided groupwise registration) can achieve much higher overlap ratio than the pairwise algorithm (HAMMER). For example, the overlap ratios of the ABSORB method can reach 79.01% in WM, 66.82% in GM, and 82.33% in VN, which achieves more than 10% improvement in the overall overlap ratio. The congealing method (a hidden common space based groupwise registration method), however, is not as good as the pairwise counterpart (HAMMER) in terms of overlap ratios at the current stage. One possible reason for this is that much more parameters, compared with those of the pairwise registration method, are involved into the optimization of the objective function (e.g., the stack entropy in the congealing method) in this class of registration methods. In pairwise registration, only the deformation of a single image needs to be estimated, while in groupwise registration the deformations have to be simultaneously refined for all images. Thus the optimization involved in groupwise registration is more vulnerable to local minima, with the same gradient based optimization method. However, by integrating the congealing method into a hierarchical groupwise registration framework [35, 43] which only performs congealing on a set of subjects with similar appearances, the registration performance in terms of the overlap ratio can be improved drastically, as shown in the last row of Table 1.

**Table 1.** Overall overlap ratios of WM, GM, and VN by five different registration algorithms.

	White Matter	Gray Matter	Ventricle	Overall
<b>Pairwise HAMMER</b>	63.86% ( $\pm 3.87\%$ )	57.25% ( $\pm 2.18\%$ )	76.51% ( $\pm 3.70\%$ )	65.64% ( $\pm 3.15\%$ )
<b>Group Mean Method</b>	73.88%	60.51%	78.14%	70.84%
<b>ABSORB</b>	79.01%	66.82%	82.33%	76.05%
<b>Congealing Method</b>	59.68%	51.09%	70.61%	59.43%
<b>Hierarchical Congealing</b>	65.64%	58.36%	78.60%	67.54%

**Multiple Modes in Groupwise Registration:** The inter-subject variation can be so large that a single common space can barely handle the groupwise registration [68]. As discussed previously, an individual subject can be connected to the final population center by a path consisting of segments linking neighboring subjects. In ABSORB, nearby images are automatically bundled together in the self-organized registration progress. A single representative image is selected from each bundle to participate into the further registration in the higher level. In general, images in a population can be better represented by multiple modes. By taking advantage of the multiple mode phenomena, groupwise registration could become more accurate and efficient.

In Wang et al. [35, 43], all subjects are hierarchically clustered according to the specific pairwise similarity or distance definition. The top-down hierarchical clustering yields a pyramid, where each leaf node corresponds to an image in the population. In each class, subjects are close to each other. Then registration is always intra-class, as only the images in the identical class are warped to the center of the class in groupwise registration manner. Similar to ABSORB, only a single subject will be produced to represent the whole class when intra-class registration has finished, and contribute to registration in the higher level. From the perspective of the pyramid, the task of intra-class registration happens from the bottom of the pyramid, then climbs up, and finally ends at the top. Meanwhile, all images in the population are warped to the common space, following the path from its corresponding leaf node to the root of the pyramid. In each intra-class registration, subjects involved are much less diverse than the whole population. Therefore, to perform groupwise registration on a class of images is much easier and more accurate than to perform groupwise registration of all images directly. Moreover, the whole computation load is dispatched into several classes where only a small number of subjects are handled, leading to a faster registration algorithm.

An example with only three levels is shown in Fig. 11, where groupwise registration has been performed on 150 brain MR images. For clarity, only a few subjects are displayed here. In the first level, each class contains a very limited number of subjects, which are quite close to each other. Then intra-class registration yields the representative image for the respective class. And in the second level, intra-class registrations perform again, resulting in fewer modes of the population. The whole process ends in the third level, where a single representative for the whole population is produced. For each image at the leaf node, it can be warped to the common space, following its individual path from the leaf node to the root node of the pyramid.

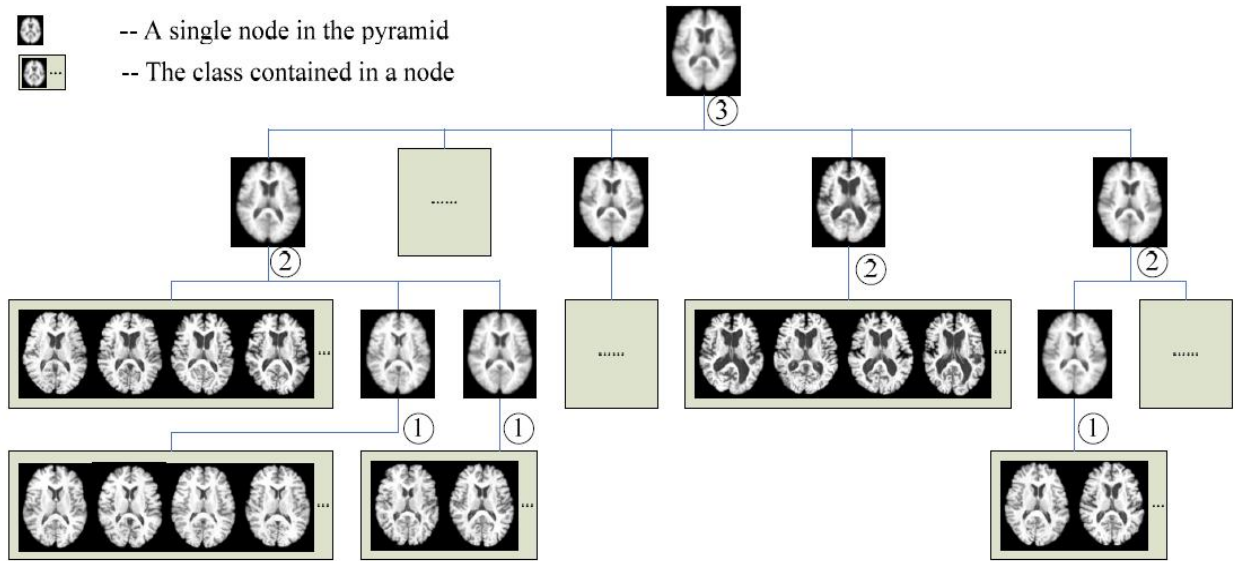


**Fig. 11.** An image population of 150 brain MR images is hierarchically clustered into a pyramid, based on the similarity definition between any two images [43]. Groupwise registration is performed in each class, producing the representative image for the class (label ①). The representative images participate into intra-class registrations in the higher level (label ②). Finally, a single representative is estimated (label ③), as the whole registration process reaches the top of the pyramid. Each input image then can be warped to the common space by following its respective deformation path.

Groupwise registration can be employed to explore the existence of multiple modes in an image population. Sabuncu et al. [31] incorporated the groupwise registration into a generalized EM framework. Each subject is assigned a label. The assignments are refined, as images of the same label are warped together in a groupwise registration manner. And after the EM process converges, the

intrinsic multiple modes of the image population are naturally manifested. For example, they can discriminate the subjects from different age groups.

**Atlas building for infants:** Atlas, which refers to a map or spatial record of what we know about a region, is widely used in many disciplines and applications. Brain atlases usually refer to the images incorporated with prior knowledge and take the forms of, for example, an averaged intensity model of the population, as well as the tissue probability maps of WM, GM and CSF. In many applications, researchers use these atlases as registration templates in spatial normalization, and also as prior knowledge for guiding tissue segmentation. Atlas building is more important and challenging in infant image analysis than in adult because of the poor spatial resolution, low tissue contrast, and high within-tissue intensity variability of the MR images [55, 56, 66]. An atlas with average-shape can normalize an infant population into the same space, and the prior probability maps can guide the tissue segmentation of infant population, which can be eventually used to disclose the brain development in the infant stage.

To build the infant atlas, we use a longitudinal dataset, in which MR scans were acquired longitudinally in neonates, 1 year old, and 2 years old [45]. We then employ the state-of-the-art longitudinal segmentation and groupwise registration methods to build infant atlases.

This dataset was collected as one of our longitudinal studies, involving 56 infants (27 males and 29 females). Each subject has a set of MR brain images scanned at 3 time points, as neonates ( $0.9 \pm 0.3$  months), 1 year old ( $13.2 \pm 0.7$  months), and 2 years old ( $24.9 \pm 1.9$  months). These healthy subjects were recruited from UNC-CH and are free of congenital anomalies, metabolic disease, and focal lesions. Informed consent was obtained from the parents and the experimental protocols were approved by the institutional review board. All subjects were unmedicated during MR imaging.

For each subject, T1 and T2 MR brain images were collected using a 3T Siemens scanner. For T1 images, 160 sagittal slices were obtained with parameters: TR=1900ms, TE=4.38ms, Flip Angle=7, and resolution= $1 \times 1 \times 1$  mm<sup>3</sup>. For T2 images, 70 transverse slices were acquired with parameters: TR=7380ms, TE=119ms, Flip Angle=150, and resolution= $1.25 \times 1.25 \times 1.95$  mm<sup>3</sup>.

All images are preprocessed utilizing a standard pipeline. To achieve better tissue contrast, T2 is selected for neonate, and T1 is selected for 1 year old and 2 years old. T2 images are resampled into  $1 \times 1 \times 1 \text{ mm}^3$ . Non-brain tissues (such as skull and dura) are stripped with Brain Surface Extractor (BSE) [69], followed by manual editing in ITK-SNAP software [70] to ensure accurate removal. Bias correction is performed in all images with N3 method [71] to reduce the impact of intensity inhomogeneity and thus improve the performance of the subsequent segmentation and registration.

We employ the strategy proposed in [45] to first segment the last time-point image, and then take advantage of the longitudinal follow-up time-point to build a subject-specific tissue probabilistic atlas including WM, GM, and CSF, to guide the earlier time-point segmentation, which has much lower tissue contrast. In particular, the T1 image of 2 years old subjects has shown the early adult pattern, and tissue structures can be well segmented with fuzzy segmentation technique such as adaptive K-means algorithm [72]. Then the tissue probability maps of 2 years old subjects are warped into neonate and 1 year old subjects separately and serve as prior to guide their tissue segmentations. The segmentation results are used to refine the registration to better warp the probability maps of 2 years old subjects to the current time-point. With better prior, the performance of the segmentation can be improved. This joint registration-segmentation iterates until convergence. This technique can substantially improve the tissue segmentation accuracy of infant brain images, especially for neonates. After this procedure, the tissue probability maps for all images are obtained.

Next, we build the average-shape atlas for each age group, including the intensity model and the probability maps for WM, GM, and CSF. The conventional atlas building algorithm selects a subject image from or out of this population to be the template. The atlas constructed is anatomically similar with the selected template and is hence biased. Unbiased registration is more preferable here for determining an atlas which is able to better represent the anatomy of the whole population. We employ the groupwise registration method proposed in [41] for unbiased groupwise atlas building. This groupwise registration algorithm utilizes the attribute vector as the morphological signature to robustly identify the anatomical correspondences. Therefore, more accurate registration results can be achieved compared to the intensity based algorithms.

We show the constructed average-shape atlases for 0, 1, and 2 years in Fig. 12. The anatomical proportion of 0-1-2 years is preserved and can be observed from the figure. With these constructed

atlases, we now have the tissue probability for the specific age range of infants. We can use these atlases for guiding the segmentation of neonates with missing longitudinal data in the 1 year old or 2 years old, as we did in [65].The atlases are freely available to the research community at <http://bric.unc.edu/ideagroup/free-softwares/>.

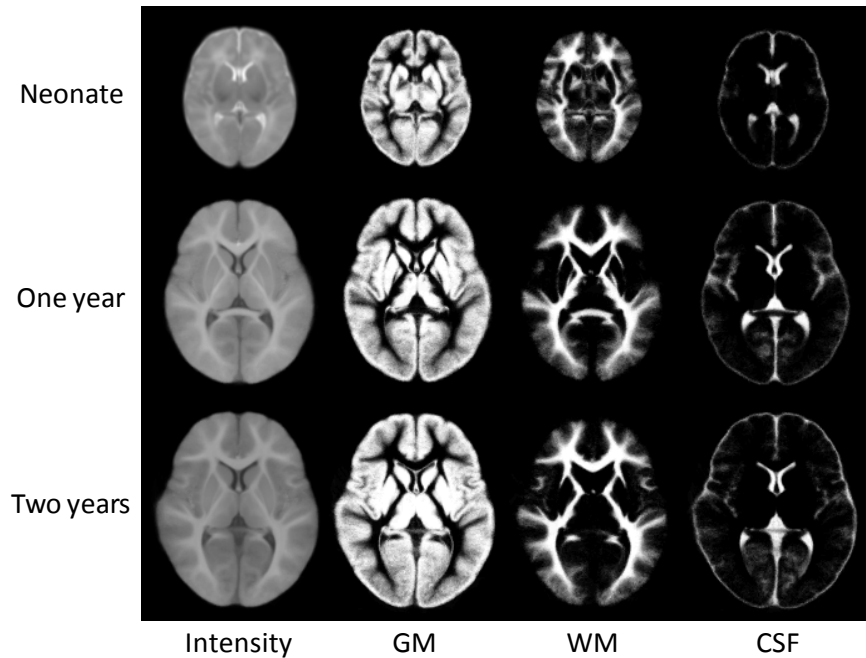


**Fig. 12.** Illustration of the average-shape atlases of 0-1-2 years. The intensity model and tissue probability maps of WM, GM, and CSF are shown, respectively.

## 6. Summary

In past decades, image registration has been proven to be important for effective medical image analysis. By normalizing an image population to the same space by image registration, qualitative and quantitative analysis on brain anatomies and morphologies can be performed. Plenty of applications have been explored, ranging from brain development study to early disease diagnosis. To meet the booming requirement for the unbiased group analysis, a relatively new family of registration methods, called as groupwise registration has come to the stage. As demonstrated in various applications, groupwise registration algorithms generally demonstrate superior performance over their pairwise counterparts, and thus becomes a hot topic in the field of medical image analysis.

## Reference

- [1] E. M. Haacke, R. F. Brown, M. Thompson, and R. Venkatesan, *Magnetic resonance imaging: physical principles and sequence design*. New York: J. Wiley & Sons, 1999.
- [2] J. B. A. Maintz and M. A. Viergever, "A survey of medical image registration," *Medical Image Analysis*, vol. 2, pp. 1-36, 1998.
- [3] B. Zitová and J. Flusser, "Image registration methods: a survey," *Image and Vision Computing*, vol. 21, pp. 977-1000, 2003.
- [4] W. R. Crum, T. Hartkens, and D. L. G. Hill, "Non-rigid image registration: theory and practice," *British Journal of Radiology*, vol. 77, pp. S140-153, 2004.
- [5] R. P. Woods, S. T. Grafton, C. J. Holmes, S. R. Cherry, and J. C. Mazziotta, "Automated image registration: I. General methods and intrasubject, intramodality validation," *Journal of Computer Assisted Tomography*, vol. 22, pp. 139-152, 1998.
- [6] R. P. Woods, S. T. Grafton, J. D. G. Watson, N. L. Sicotte, and J. C. Mazziotta, "Automated image registration: II. Intersubject validation of linear and nonlinear models," *Journal of Computer Assisted Tomography*, vol. 22, pp. 153-165, 1998.
- [7] S. Joshi and M. I. Miller, "Landmark matching via large deformation diffeomorphisms," *IEEE Transactions on Medical Imaging*, vol. 9, pp. 1357-1370, 2000.
- [8] Z. Xue, D. Shen, and C. Davatzikos, "Determining correspondence in 3D MR brain images using attribute vectors as morphological signatures of voxels," *Medical Imaging, IEEE Transactions on*, vol. 23, pp. 1276-1291, 2004.
- [9] P. J. Besl and H. D. McKay, "A method for registration of 3-D shapes," *Pattern Analysis and Machine Intelligence, IEEE Transactions on*, vol. 14, pp. 239-256, 1992.
- [10] T. Vercauteren, X. Pennec, A. Perchant, and N. Ayache, "Diffeomorphic demons: efficient non-parametric image registration," *NeuroImage*, vol. 45, pp. S61-S72, 2009.
- [11] D. Rueckert, L. I. Sonoda, C. Hayes, D. L. G. Hill, M. O. Leach, and D. J. Hawkes, "Nonrigid registration using free-form deformations: application to breast MR images," *Medical Imaging, IEEE Transactions on*, vol. 18, pp. 712-721, 1999.
- [12] J. P. Thirion, "Image matching as a diffusion process: an analogy with Maxwell's demons," *Medical Image Analysis*, vol. 2, pp. 243-260, 1998.
- [13] M. I. Miller, "Computational anatomy: shape, growth, and atrophy comparison via diffeomorphisms," *NeuroImage*, vol. 23, pp. S19-S33, 2004.
- [14] J. Ashburner, "A fast diffeomorphic image registration algorithm," *NeuroImage*, vol. 38, pp. 95-113, 2007.
- [15] G. E. Christensen and H. J. Johnson, "Consistent image registration," *Medical Imaging, IEEE Transactions on*, vol. 20, pp. 568-582, 2001.
- [16] D. Shen, "Image registration by local histogram matching," *Pattern Recognition*, vol. 40, pp. 1161-1172, 2007.
- [17] D. Shen and C. Davatzikos, "HAMMER: Hierarchical attribute matching mechanism for elastic registration," *Medical Imaging, IEEE Transactions on*, vol. 21, pp. 1421-1439, 2002.
- [18] D. Shen and C. Davatzikos, "Very high-resolution morphometry using mass-preserving deformations and HAMMER elastic registration," *NeuroImage*, vol. 18, pp. 28-41, 2003.
- [19] G. Wu, P.-T. Yap, M. Kim, and D. Shen, "TPS-HAMMER: Improving HAMMER registration algorithm by soft correspondence matching and thin-plate splines based deformation interpolation," *NeuroImage*, vol. 49, pp. 2225-2233, 2010.

- [20] C. H. Lo and H. S. Don, "3-D moment forms: their construction and application to object identification and positioning," *Pattern Analysis and Machine Intelligence, IEEE Transactions on*, vol. 11, pp. 1053-1064, 1989.
- [21] S. M. Resnick, A. F. Goldszal, C. Davatzikos, S. Golski, M. A. Kraut, E. J. Metter, R. N. Bryan, and A. B. Zonderman, "One-year age changes in MRI brain volumes in older adults," *Cerebral Cortex*, vol. 10, pp. 464-472, 2000.
- [22] Z. Lao, D. Shen, Z. Xue, B. Karacali, S. M. Resnick, and C. Davatzikos, "Morphological classification of brains via high-dimensional shape transformations and machine learning methods," *Neuroimage*, vol. 21, pp. 46-57, 2004.
- [23] A. W. Toga and P. M. Thompson, "The role of image registration in brain mapping," *Image and Vision Computing*, vol. 19, pp. 3-24, 2001.
- [24] H. Park, P. H. Bland, A. O. Hero, and C. R. Meyer, "Least biased target selection in probabilistic atlas construction," in *Medical Image Computing and Computer-Assisted Intervention – MICCAI 2005*, 2005, pp. 419-426.
- [25] D. Seghers, E. D'Agostino, F. Maes, D. Vandermeulen, and P. Suetens, "Construction of a brain template from MR images using state-of-the-art registration and segmentation techniques," in *Medical Image Computing and Computer-Assisted Intervention – MICCAI 2004*, 2004, pp. 696-703.
- [26] S. Joshi, B. Davis, M. Jomier, and G. Gerig, "Unbiased diffeomorphic atlas construction for computational anatomy," *NeuroImage*, vol. 23, pp. S151-S160, 2004.
- [27] J. Hamm, C. Davatzikos, and R. Verma, "Efficient large deformation registration via geodesics on a learned manifold of images," London, UK, 2009.
- [28] E. G. Learned-Miller, "Data driven image models through continuous joint alignment," *Pattern Analysis and Machine Intelligence, IEEE Transactions on*, vol. 28, pp. 236-250, 2006.
- [29] L. Zöllei, E. Learned-Miller, E. Grimson, and W. Wells, "Efficient population registration of 3D data," in *Computer Vision for Biomedical Image Applications (ICCV)*, 2005, pp. 291-301.
- [30] S. K. Balci, P. Golland, M. Shenton, and W. M. Wells, "Free-form B-spline deformation model for groupwise registration," in *Medical Image Computing and Computer-Assisted Intervention – MICCAI 2007*, 2007, pp. 23-30.
- [31] M. R. Sabuncu, S. K. Balci, M. E. Shenton, and P. Golland, "Image-driven population analysis through mixture modeling," *Medical Imaging, IEEE Transactions on*, vol. 28, pp. 1473-1487, 2009.
- [32] H. Jia, G. Wu, Q. Wang, and D. Shen, "ABSORB: Atlas building by self-organized registration and bundling," in *IEEE Conference on Computer Vision and Pattern Recognition*, San Francisco, CA, 2010.
- [33] H. Jia, G. Wu, Q. Wang, and D. Shen, "ABSORB: Atlas building by self-organized registration and bundling," *NeuroImage*, accepted, 2010.
- [34] F. Wang, B. C. Vemuri, A. Rangarajan, and S. J. Eisenschenk, "Simultaneous nonrigid registration of multiple point sets and atlas construction," *Pattern Analysis and Machine Intelligence, IEEE Transactions on*, vol. 30, pp. 2011-2022, 2008.
- [35] Q. Wang, L. Chen, and D. Shen, "Group-wise registration of large image dataset by hierarchical clustering and alignment," in *Medical Imaging 2009*. vol. 7259: SPIE, 2009.
- [36] Q. Wang, P.-T. Yap, G. Wu, and D. Shen, "Attribute vector guided groupwise registration," in *Medical Image Computing and Computer-Assisted Intervention – MICCAI 2009*, 2009.
- [37] Q. Wang, G. Wu, P.-T. Yap, and D. Shen, "Attribute vector guided groupwise registration," *NeuroImage*, vol. 50, pp. 1485-1496, 2010.

- [38] S. Marsland, C. J. Twining, and C. J. Taylor, "A minimum description length objective function for groupwise non-rigid image registration," *Image and Vision Computing*, vol. 26, pp. 333-346, 2008.
- [39] S. Marsland and C. J. Twining, "Constructing diffeomorphic representations for the groupwise analysis of nonrigid registrations of medical images," *Medical Imaging, IEEE Transactions on*, vol. 23, pp. 1006-1020, 2004.
- [40] P. T. Fletcher, S. Venkatasubramanian, and S. Joshi, "The geometric median on Riemannian manifolds with application to robust atlas estimation," *NeuroImage*, vol. 45, pp. S143-S152, 2009.
- [41] G. Wu, P.-T. Yap, Q. Wang, and D. Shen, "Groupwise registration from exemplar to group mean: extending HAMMER to groupwise registration," in *ISBI 2010 The Netherlands*, 2010.
- [42] B. C. Munsell, A. Temlyakov, and S. Wang, "Fast multiple shape correspondence by pre-organizing shape instances," in *IEEE Conference on CVPR*, 2009, pp. 840-847.
- [43] Q. Wang, L. Chen, P. T. Yap, G. Wu, and D. Shen, "Groupwise registration based on hierarchical image clustering and atlas synthesis," *Human Brain Mapping*, accepted, 2010.
- [44] E. G. Miller, N. E. Matsakis, and P. A. Viola, "Learning from one example through shared densities on transforms," in *Computer Vision and Pattern Recognition, 2000. Proceedings. IEEE Conference on*, 2000, pp. 464-471
- [45] F. Shi, Y. Fan, S. Tang, J. H. Gilmore, W. Lin, and D. Shen, "Neonatal brain image segmentation in longitudinal MRI studies," *NeuroImage*, vol. 49, pp. 391-400, 2010.
- [46] T. Cox and M. A. A. Cox, *Multidimensional scaling*, second ed. London: Chapman & Hall, 2000.
- [47] S. Baloch and C. Davatzikos, "Morphological appearance manifolds in computational anatomy: Groupwise registration and morphological analysis," *NeuroImage*, vol. 45, pp. S73-S85, 2009.
- [48] S. Baloch, R. Verma, and C. Davatzikos, "An anatomical equivalence class based joint transformation-residual descriptor for morphological analysis," in *Information Processing in Medical Imaging*, 2007, pp. 594-606.
- [49] S. Tang, Y. Fan, and D. Shen, "RABBIT: Rapid alignment of brains by building intermediate templates," *NeuroImage*, vol. 47, pp. 1277-1287, 2009.
- [50] M.-J. Kim, M.-H. Kim, and D. Shen, "Learning-based deformation estimation for fast non-rigid registration," in *2008 IEEE Conference on Computer Vision and Pattern Recognition Workshops Anchorage, Alaska*, 2008, pp. 1-6.
- [51] J. B. Kruskal, "On the shortest spanning subtree of a graph and the traveling salesman problem," *Proceedings of the American Mathematical Society*, vol. 7, pp. 48-50, 1956.
- [52] K. K. Bhatia, J. V. Hajnal, B. K. Puri, A. D. Edwards, and D. Rueckert, "Consistent groupwise non-rigid registration for atlas construction," in *IEEE Int. Symp. Biomed. Imag.: Macro Nano*, 2004. vol. 1, 2004, pp. 908-911.
- [53] J. Lin, "Divergence measures based on the shannon entropy," *Information Theory, IEEE Transactions on*, vol. 37, pp. 145-151, 1991.
- [54] R. Wolz, P. Aljabar, J. V. Hajnal, A. Hammers, and D. Rueckert, "LEAP: Learning embeddings for atlas propagation," *NeuroImage*, vol. 49, pp. 1316-1325, 2010.
- [55] R. C. Knickmeyer, S. Gouttard, C. Kang, D. Evans, K. Wilber, J. K. Smith, R. M. Hamer, W. Lin, G. Gerig, and J. H. Gilmore, "A structural MRI study of human brain development from birth to 2 years," *J Neurosci*, vol. 28, pp. 12176-82, 2008.
- [56] W. Gao, H. Zhu, K. S. Giovanello, J. K. Smith, D. Shen, J. H. Gilmore, and W. Lin, "Evidence on the emergence of the brain's default network from 2-week-old to 2-year-old healthy pediatric subjects," *Proc Natl Acad Sci U S A*, vol. 106, pp. 6790-6795, 2009.

- [57] C. Hutton, E. De Vita, J. Ashburner, R. Deichmann, and R. Turner, "Voxel-based cortical thickness measurements in MRI," *Neuroimage*, vol. 40, pp. 1701-10, 2008.
- [58] S. R. Das, B. B. Avants, M. Grossman, and J. C. Gee, "Registration based cortical thickness measurement," *Neuroimage*, vol. 45, pp. 867-879, 2009.
- [59] ADNI, "<http://www.loni.ucla.edu/ADNI/>," 2004.
- [60] P.-T. Yap, G. Wu, H. Zhu, W. Lin, and D. Shen, "Fast tensor image morphing for elastic registration," in *Medical Image Computing and Computer-Assisted Intervention – MICCAI 2009*, 2009, pp. 721-729.
- [61] P.-T. Yap, G. Wu, H. Zhu, W. Lin, and D. Shen, "TIMER: Tensor image morphing for elastic registration," *NeuroImage*, vol. 47, pp. 549-563, 2009.
- [62] P. Hagmann, L. Cammoun, X. Gigandet, R. Meuli, C. J. Honey, V. J. Wedeen, and O. Sporns, "Mapping the structural core of human cerebral cortex," *PLoS Biol*, vol. 6, pp. 1479-1493, 2008.
- [63] C. Davatzikos, Y. Fan, X. Wu, D. Shen, and S. M. Resnick, "Detection of prodromal alzheimer's disease via pattern classification of MRI," *Neurobiology of Aging*, vol. 29, pp. 514-523, 2008.
- [64] F. Shi, D. Shen, P.-T. Yap, Y. Fan, J. Cheng, H. An, L. L. Wald, G. Gerig, J. H. Gilmore, and W. Lin, "CENTS: Cortical enhanced neonatal tissue segmentation," *Human Brain Mapping*, accepted, 2010.
- [65] F. Shi, P.-T. Yap, J. H. Gilmore, W. Lin, and D. Shen, "Construction of multi-region-multi-reference atlases for neonatal brain MRI segmentation," *NeuroImage*, accepted, 2010.
- [66] M. Altabe, S. K. Holland, M. Wilke, and C. Gaser, "Infant brain probability templates for MRI segmentation and normalization," *Neuroimage*, vol. 43, pp. 721-30, 2008.
- [67] P. Jaccard, "The distribution of the flora in the alpine zone," *New Phytologist*, vol. 11, pp. 37-50, 1912.
- [68] D. J. Blezek and J. V. Miller, "Atlas stratification," *Medical Image Analysis*, vol. 11, pp. 443-457, 2007.
- [69] D. W. Shattuck and R. M. Leahy, "Automated graph-based analysis and correction of cortical volume topology," *IEEE Transactions on Medical Imaging*, vol. 20, pp. 1167-77, Nov 2001.
- [70] P. A. Yushkevich, J. Piven, H. C. Hazlett, R. G. Smith, S. Ho, J. C. Gee, and G. Gerig, "User-guided 3D active contour segmentation of anatomical structures: Significantly improved efficiency and reliability," *Neuroimage*, vol. 31, pp. 1116-1128, 2006.
- [71] J. G. Sled, A. P. Zijdenbos, and A. C. Evans, "A nonparametric method for automatic correction of intensity nonuniformity in MRI data," *IEEE Trans Med Imaging*, vol. 17, pp. 87-97, Feb 1998.
- [72] D. L. Pham and J. L. Prince, "An adaptive fuzzy C-means algorithm for image segmentation in the presence of intensity inhomogeneities," *Pattern Recognition Letters*, vol. 20, pp. 57-68, 1999.